Journal of Applied Mechanics and Technical Physics, Vol. 41, No. 1, 2000

THE FLOW IN A PLANAR-RADIAL VORTEX CHAMBER.

2. VORTEX STRUCTURE OF THE FLOW

F. A. Bykovskii and E. F. Vedernikov

UDC 532.527+536.37

A vortex structure of an air flow with a characteristic size of vortices comparable with the primary vortex size was observed in a vortex chamber of planar–radial geometry for the first time. The vortex component of the flow velocity along the chamber radius and its axis was calculated.

The flow structure in rotating flows is of interest for many researchers studying the Ranque effect [1]. To explain the heating of peripheral layers of a gas in swirled flows, the notion of vortex moles is introduced. A chain consisting of these moles transfers the energy of the lower layers of the flow to the upper layers. According to Merkulov and Kudryavtsev [2], the motion of vortices to the neighboring region of the flow and back is the reason for elementary Carnot cycles and, hence, heat exchange between the layers. The temperature distribution observed is mathematically described by means of these vortex moles [3]. Nevertheless, the authors are unaware of any experimental confirmation of the existence of hypothetical vortex moles. The first attempt to interpret the vortex structures seems to have been undertaken by Lukachev [4, 5]. According to these papers, rotating helical structures of shear nature, which call forth the precession of the axial flow, are formed at the boundary of peripheral and axial flows. Radial oscillations of the axial flow result in pseudoturbulence of the flow periphery and an onset of heat transfer. A vortex structure of the flow in the form of helical streets was found in a short chamber [6].

Our investigations of the flow in a planar-radial vortex chamber whose diameter is much greater than its height ($d_{ch} \gg Z$) confirm the vortex nature of the flow and allow us to determine the characteristic size of the vortices that arise in the primary vortex and have dimensions comparable with the latter.

The experimental chamber and corresponding devices are described in [7]. The measurement techniques for the mean velocity $\langle u \rangle$ in the flow along the chamber radius r and axis z in the transient and steady regimes are also described in the same paper. The flow was analyzed using the measurement of the total P_0 and static P pressures over the entire volume of the chamber.

Pressure Measurement. The construction of the probes is shown in Fig. 1. Case 1 contains a glass with membrane 3 with glued semiconductor strain-gauge probe 2 with a base of 2 mm, which is included into the bridge circuit of measurement. To stabilize the temperature of the strain-gauge probe in the course of experiment and to exclude the free volume, the glass with the membrane was filled by cup grease 4. Probe sensor 5 was a tube moved out into the flow. The tube in the static-pressure probe had an open end with thin plate 6 welded onto it (Fig. 1a), and the tube of the total-pressure probe had a closed end and a lateral orifice (Fig. 1b). The end of the orifice was squared, which made it possible to rotate the probe by an angle of $\pm 30°$ relative to the flow direction, and the error of pressure measurement was less than 1.5% [8]. In some experiments, we used a tube 1 mm in diameter, which was bent opposite the flow. The probes of total and

Lavrent'ev Institute of Hydrodynamics, Siberian Division, Russian Academy of Sciences, Novosibirsk 630090. Translated from Prikladnaya Mekhanika i Tekhnicheskaya Fizika, Vol. 41, No. 1, pp. 41–49, January–February, 2000. Original article submitted March 10, 1998; revision submitted December 3, 1998.

0021-8944/00/4101-0035 $25.00

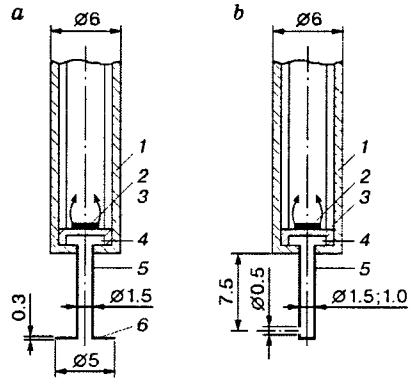

Fig. 1. Scheme of probes for static and total pressure: 1) case of the probe; 2) semiconductor strain-gauge probe; 3) membrane; 4) cup grease; 5) probe tube; 6) plate.

static pressure were located over the chamber circumference at an equal distance from the wall and 20 mm from each other and could be moved over the chamber height z.

The characteristic time of travelling of the acoustic wave in the probe tube was about 25 μsec, and the natural frequency of oscillations of the probe membrane was about 2 mHz, which allowed us to register signals with duration up to dozens of microseconds. The signals were recorded to S8-13 and S9-16 oscillographs. The S9-16 two-beam digital oscillograph allowed us to compare time intervals of the oscillograms with accuracy up to 10 μsec.

Simultaneous recording of oscillograms of the total and static pressures during the entire transient process was possible only at two points of the chamber, and the pressure along the chamber radius and height z was registered in a series of experiments. The radii along which the pressure was measured roughly coincided with the radii of injection of the products of explosion of aluminum foil by electric current [7]. The initial pressure of air of $100 \cdot 10^5$ Pa in receivers with $V_r = 3.6$ and 80 liters and the starting time of pressure recording remained constant in all experiments. Control tests for identical positions of the probes confirmed the identity of the recorded oscillograms.

The construction of the probes and the measurement scheme included everything possible to eliminate spurious oscillations. The use of semiconductor strain-gauge probes, which do not require signal amplification, the low resistance of the probes (about 200 Ω), the use of the bridging scheme, and the power fed by storage cells allowed us to avoid spurious oscillations in the measurement circuit. The probes did not respond to knocks on the case and tube and, therefore, did not register acoustic oscillations in the case of the chamber during the experiments.

In addition, control tests were conducted. In one of them, the orifices in the tubes were closed. In this case, oscillations in the vortex flow were not registered, i.e., the probe did not respond to acoustic oscillations in the chamber wall and vibration of the probe tubes. In another experiment, the cavities in the probe tubes were filled by cup grease. Pressure oscillations were eliminated due to damping by the viscous medium, and the constant component of pressure was registered.

Finally, the total pressure was measured by a tube 16 mm in diameter and 1 m long. The end diameter of the tube was twice as small to generate a subsonic flow in it. The tube was attached to the valve of the feeding system. Oscillations of lower frequency appeared when the tube was filled by air; in this case, the appearance of shock waves is inevitable after opening of the valve. After that, no oscillations were registered. On the basis of the experiments conducted, we can conclude that the probe does not respond to acoustic oscillations in the case of the chamber and to vibration of its elements and does not generate acoustic oscillations inside the probe tubes.

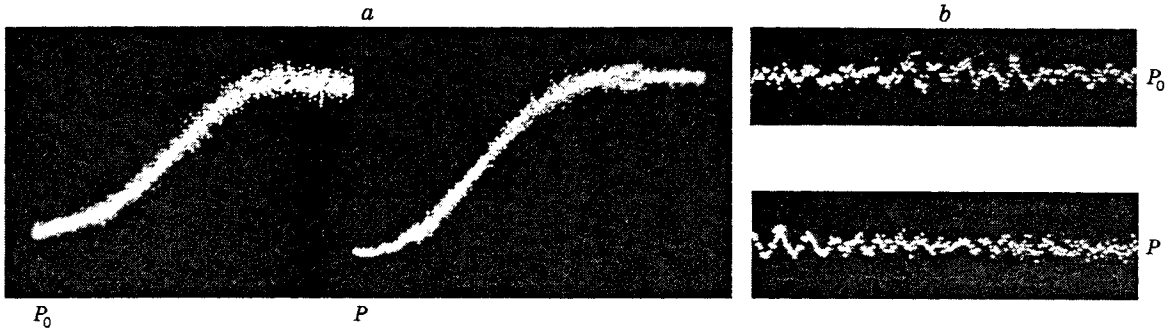

Fig. 2. Typical oscillograms of the total (P_0) and static (P) pressures during 20 msec after opening of the valves (a) and in an increased time scale (b).

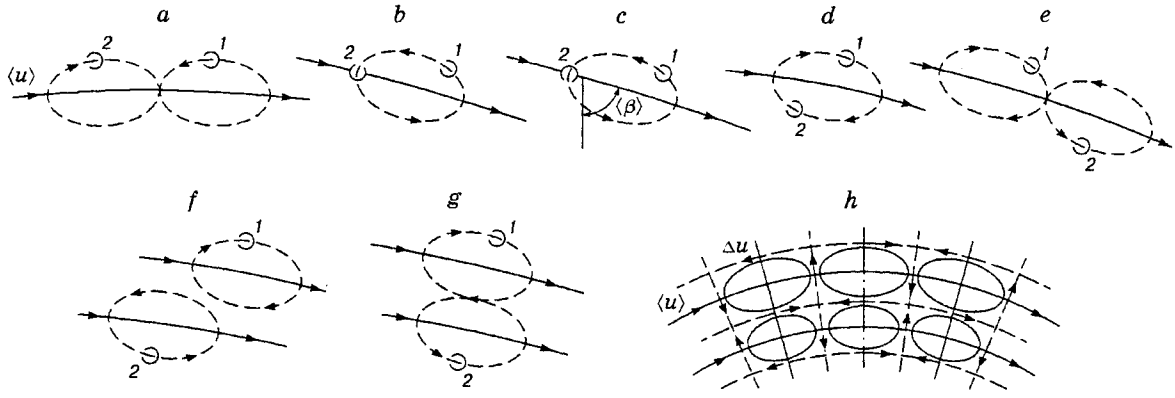

Fig. 3. Interpretation of the vortex motion in the chamber: (a–c) the probes are located at the circumference of radius $r = 80$ mm [the probes are oriented upstream (a) and probe 2 is oriented at an angle of $\pm 90°$ to the flow (b and c)]; (d and e) probe 2 is located at the circumference of radius $r = 69$ mm; (f and g) probe 2 is located at the circumference of radius $r = 60$ mm; (h) vortex flow structure.

Results of Experiments and Discussion. Typical oscillograms of P_0 and P during 20 msec after opening of the valves, which were recorded at the points $r = 80$ mm and $z = 7.5$ mm, are plotted in Fig. 2a. Figure 2b shows parts of these oscillograms with the time scale enlarged by a factor of 16. It is seen that P_0 and P experience oscillations; therefore, the gas motion is unsteady. The frequency of oscillations of P_0 and P is identical, but the oscillations of P are weaker than the oscillations of P_0. At the ends of the chamber, the oscillations of P_0 and P decrease to the noise level.

To determine the direction and phase of the velocity oscillation Δu, we used two total pressure probes. We studied the flow region in the center of the chamber ($z = 7.5$ mm) near the point $r = 80$ mm, where the greatest vorticity of the flow was observed [7]. Probe 1 remained motionless at the point $r = 80$ mm and was oriented upstream. Probe 2 with different orientations was installed near probe 1 (Fig. 3). In schemes presented in Fig. 3a–c, probe 2 was mounted at the circumference of the same radius $r = 80$ mm, but was oriented upstream, like probe 1 (Fig. 3a) or at an angle of $\pm 90°$ to the flow (Fig. 3b and c). Probe 2 was also placed at the circumferences of radii $r = 69$ mm (Fig. 3d and e) and $r = 60$ mm (Fig. 3f and g). The distance between the seats for the probes on one circumference was 20 mm. The signals from the probes were shown on an S9-16 oscillograph.

For $\langle u \rangle \approx 200$ m/sec and a half-period of oscillations $\Delta t_v/2 \approx 100$ μsec, the probes mounted as shown in Fig. 3a registered Δu in the opposing phase for all changes in $\langle \beta \rangle$, which is the angle between the direction $\langle u \rangle$ and the radius r. The probes mounted in accordance with schemes shown in Fig. 3b and c simultaneously registered oscillations for $\langle \beta \rangle < 80°$ [in the opposing (b) and coincident (c) phases]. In the schemes shown in Fig. 3d–g, Δu was registered both in the coincident and opposite phases depending on the

inclination of the streamlines. The maximum amplitudes of oscillations and their periods over the chamber circumference and radius were identical with accuracy to the amplitude and time steps of discretization, which were approximately 15% of the amplitude of oscillations and about 5% of the period of the registered signal, respectively. The presence of circumferential and radial phase-coincident oscillations close in amplitude and period on the neighboring streamlines indicates the existence of oscillating vortex structures rotating in the plane of the chamber (dashed curves in Fig. 3a–g). The characteristic size of the vortices along the streamlines is determined by the product of the half-period of oscillations and the mean flow velocity $(\Delta t_v/2)\langle u\rangle$. It is equal to 15–20 mm in the transitional flow regime in the chamber near the point $r = 80$ mm. In the steady flow regime, the characteristic size of the vortices decreases approximately to 10 mm. Along the radius, the characteristic size of the vortices is 10–15 mm; it was determined from simultaneous emergence of the maximum oscillations registered by probes 1 and 2. Thus, the mean characteristic size of the vortices is 1/10–1/20 of the primary vortex. Fluctuations to either side of these values are possible, particularly, in the course of formation of the vortex structure.

The flow pattern in the chamber is interpreted below. The probes mounted in accordance with the scheme shown in Fig. 3a register the presence of boundaries of the opposite directions of Δu at the line where probes 1 and 2 are mounted (Fig. 3h). The distance between the boundaries is determined by the vortex size along the streamline. The probes mounted in accordance with the schemes shown in Fig. 3b and c register the direction of Δu along the boundaries. The probes mounted in accordance with the schemes in Fig. 3d–g register the opposite or coincident phase when the maxima of Δu pass through probes 1 and 2. All directions of Δu were registered in the upper streamline (Fig. 3h); in the lower streamline, the radial components of Δu were not registered. Since the value of the mean radial component of velocity $\langle u_r\rangle$ is small [7], the directions of Δu along the radius should be opposing to the upper streamline. If we smooth the corners in the resultant rectangular grid of velocity directions, we obtain a pattern of the vortex flow in the plane of the chamber. The vortices can be separated by some distance from each other. This is evidenced by the gaps between the maxima or minima of P_0 or P, which are sometimes observed. The axes of the vortices are perpendicular to the plane of the chamber and move with velocity $\langle u\rangle$ along the lines, which were defined by Bykovskii and Vedernikov [7] as streamlines on the basis of the angles $\langle\beta\rangle$. In the vortex motion, they are axes of vortex stream tubes along which vortex structures move. The streamlines are wavy curves similar to a cycloid at the development of rotation of a point along a circumference with the translational velocity greater than the circumferential one.

It is seen in Fig. 2 that the amplitude of oscillations changes in value. A comparison of the oscillations of P_0 and P shows that their amplitude within the time interval considered is not related to the vortex strength but is caused by the change in the direction of the vortex stream tubes. Most frequently, this is observed in the transient regime. Therefore, the phase of oscillations can be compared only at certain time instants, though this is quite sufficient to construct a rough flow pattern. In the region between four neighboring vortices, smaller vortices can be located, which are not registered by the available probes. In all experiments with simultaneous measurements of P_0 and P, the following picture was observed: when the probe of P_0 registers the maximum oscillations, the readings of the probe of P are minimum, and vice versa (see Fig. 2b). In the first case, vortex peripheries pass through the probes that measure P_0 and P; in the second case, vortex centers. The oscillations of P correspond to pressure variations over the vortex diameter due to centrifugal forces.

The vortex flow with the considered ratios of oscillation amplitudes to phases is most clearly identified in the steady regime ($V_r = 80$ liters) in the region $r > (2/3)R$ (R is the chamber radius), where the core flow approaches quasi-solid rotation [7]. In the region of the potential vortex ($r = 40$ mm), a comparison of oscillation amplitudes and phases shows that the vortex flow becomes less regular with predominance of small-scale oscillations, which are apparently related to splitting of large-scale vortices.

A vortex flow is also detected by the trajectories of burning aluminum particles on a stationary film. Some trajectories have a wavy shape that resembles a cycloid (Fig. 4a). The irregularity of appearance of

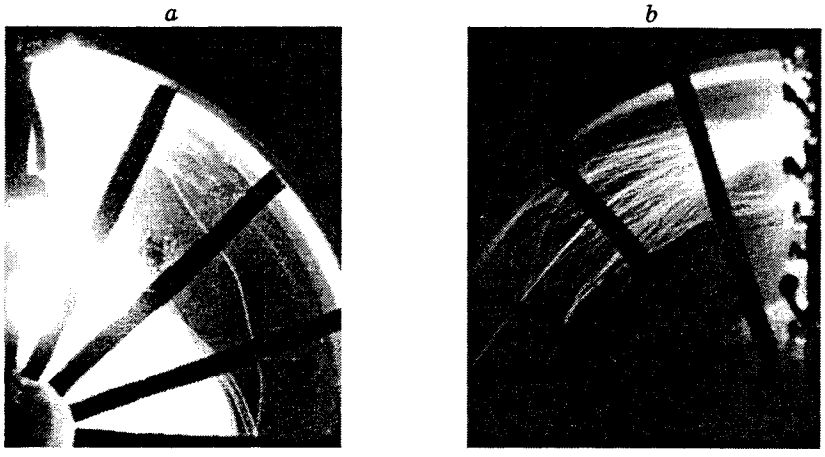

Fig. 4. Pattern of the vortex motion over the tracks of burning aluminum particles: (a) particle trajectory; (b) alternation of wide and narrow bunches of trajectories.

these trajectories is quite obvious. For a particle to repeat the path of the ambient air particles, their densities should be equal. Obviously, there are few such particles in the flow core: because of different densities, the particles heavier than air concentrate near the wall in the region of the butt-end boundary layer [7]. A wavy trajectory can be induced by the fact that the particle from the core flow enters and leaves the butt-end boundary layer many times. The closeness of the wave periods and vortex revolutions indicate the existence of the latter, which can be responsible for these transitions. Wavy trajectories were not observed when the vortex flow was not formed yet (the time of beginning of the transient regime is up to 8 msec). Numerous wavy trajectories are observed in the steady regime in the region $r > (2/3)R$, where the velocities in the flow core and in the butt-end boundary layer are close but have different directions [7].

Vortex dimensions comparable with the primary vortex size and the high value of the vortex component of velocity Δu should affect the angle of deflection of aluminum particles leaving the orifices. If the time of their outgoing is greater than 0.1 msec and the axes of the vortices pass through the orifice, the stationary film should register a bunch of trajectories with the bisectrix of its angle pointing to the mean direction of the flow. If the boundary of the vortices passes through the orifice, a narrow compact bunch of trajectories is registered. Indeed, both wide and narrow bunches of trajectories leaving the neighboring orifices were often observed in one experiment. For a 0.5-mm diameter of the orifice through which aluminum particles were thrown into the flow in the plane of the chamber at a distance of 5 mm from the wall, a dramatic increase in the bunch size was observed. At a downstream distance of 20 mm from the orifice, the bunch sometimes expanded to 10–15 mm, which corresponded to the radial size of the vortex registered by the total pressure probes (Fig. 4b). The bunch of trajectories is also formed during flow reconstruction, when the angle $\langle\beta\rangle$ changes as the aluminum particles leave the orifices. However, a dramatic expansion of the bunch near the orifice may not take place, and statistical treatment of the experimental material is necessary to reveal the flow reconstruction.

The interpreted vortex pattern in the region $r > (2/3)R$ is similar to vortex structures found previously [9–11]. In [9, 10], they were observed in a cylindrical volume of a fluid rotating as a solid body upon axial perturbations imposed on it. Axial oscillations of velocity were also present in the fluid. In our case, we did not observe axial oscillations of velocity. They could be accepted by the static pressure probes, but the estimates based on oscillation periods yield values close to $\langle u\rangle$. Transportation of the whole mass of air from one wall to the other with these velocities without sources of axial perturbations seems to be impossible. Apparently, axial oscillations of velocity cannot be excluded, but they should have lower frequencies and amplitudes, which cannot be extracted from available oscillograms.

In the experiments of Akhmetov and Tarasov [11], the vortex structure was observed in a fluid between rotating disks. Deformation of the vortex core in the form of a regular polygon was observed in some regimes. A similar deformation can also be assumed to occur in our case. In accordance with the characteristic size of oscillating structures equal, for example, to 20 mm, the primary vortex in the region $r = 80$ mm should be a rotating polygon with the number of sides roughly equal to 24. A total pressure probe with a squared inlet orifice does not register such a deformation of the vortex, since the velocity vectors change the direction only by 7.5°. In addition, it was found that the flow near the outlet orifice is supersonic even in the steady regime, and small perturbations cannot penetrate into the vortex periphery. Therefore, the deformation of the vortex core, if it exists, does not determine the character of the oscillating component of pressure.

The question can arise whether the oscillations of P_0 and P are perturbations introduced into the flow by the probes themselves. It is known that the frequency of vortices in von Kármán streets formed in the flow around cylinders is determined by the dependence $f = \mathrm{Sr}\langle u\rangle/D$ [12], where Sr is the Strouhal number and D is the cylinder diameter. For a flow velocity $\langle u\rangle = 200$ m/sec, diameter of the pressure-probe tube $D = 1$ mm, $\mathrm{Sr} = 0.21$, and Reynolds number $\mathrm{Re} > 10^3$, we obtain $f = 40$ kHz. This frequency is the limit of sensitivity of the pressure probe. In the experiment, the probes register oscillations of P_0 and P with $\Delta t_\mathrm{v} \approx 2 \cdot 10^{-4}$ sec or $f \approx 5$ kHz, which is lower than the vortex shedding frequency by an order of magnitude. Moreover, dissipation of the shed vortices occurs downstream. The characteristic time of decay of the circumferential velocity of the vortices can be estimated by the formula $t = r_\mathrm{v}^2/(4\nu)$ [13], where r_v is the vortex radius and ν is the kinematic viscosity of air. For $r_\mathrm{v} \approx (1/4)D = 0.25$ mm and $\nu = 13 \cdot 10^{-6}$ m^2/sec, we have $t = 1.2 \cdot 10^{-3}$ sec. For $\langle u\rangle = 200$ m/sec, the vortex decays at a distance of approximately 24 cm and does not affect the probe inducing it. Taking into account that pressure oscillations are already registered if the probes are located at a distance of 0.5–1.0 mm from the wall, the effect of the probes on vortex-structure formation is little probable.

The effect of the pressure probes on the flow parameters was studied by Smul'skii [14] who found that the error in pressure measurement in the chamber outside the outlet orifice is less than 1.5% for $R/R_1 = 5.2$, where R_1 is the outlet orifice radius. Indeed, if one of the probes is removed, the pressure recording made by the remaining probe does not differ from its recording made when two probes were operating. Moreover, the probes moved into the flow at a distance up to 6 mm, which is necessary to locate the orifices of the probe tubes at the opposite wall of the chamber, did not lead to noticeable changes in pressures measured with an increased length of the tubes.

The maximum value of Δu can be estimated using the equation of motion and replacing the derivatives by the ratios of the final increments $\Delta u_\mathrm{t}/\Delta t + u_r u_\mathrm{t}/r = -(1/\rho)\Delta P/(r\Delta\theta)$, where $u_\mathrm{t} = \langle u_\mathrm{t}\rangle \pm \Delta u_\mathrm{t}$ is the tangential component of the flow velocity, $\langle u_\mathrm{t}\rangle$ is the mean value of the tangential component of the flow velocity, Δu_t is its vortex component, u_r is the radial component of the flow velocity, Δt, $\Delta\theta$, and ΔP are the increments of time, angular coordinate, and static pressure, respectively, and ρ is the flow density. For example, substituting the known values for the steady regime $r = 80$ mm, $\Delta t = \Delta t_\mathrm{v}/4 \approx 0.5 \cdot 10^{-4}$ sec, $\langle u_\mathrm{t}\rangle = 80$ m/sec, $u_r = 0.15 u_\mathrm{t}$, $\rho = 53.4$ kg/m^3, $\Delta P = 1.5 \cdot 10^5$ Pa, $r\Delta\theta = 0.5 \cdot 10^{-2}$ m (half of the characteristic length of the vortex), and $\langle\beta\rangle = 82°$, we obtain $\Delta u_\mathrm{t} \approx \Delta u = 29$ m/sec.

The experimental data available do not allow one to calculate the exact distribution of the vortex component of velocity Δu over the vortex radius, but the maximum value of Δu can be calculated. For this purpose, one has to use the extreme values of P_0 and P. It is convenient to compare them in time; in this case, we have $du/dt = 0$ (see Fig. 3). The value of the derivative, which is little different from zero, is retained in a certain region; the greater the period of oscillations, the greater the size of this region. For available flow velocities, the time of the flow around a probe 1 mm in diameter is smaller than the period of pressure oscillations by a factor of 20–40. In addition, the pressure is measured in the free stream rather than in the wake behind an obstacle, and the time of flow stabilization behind the probe can be ignored. Hence, the flow around the probe with extreme values of P_0 and P can be assumed to be steady, and we can use the

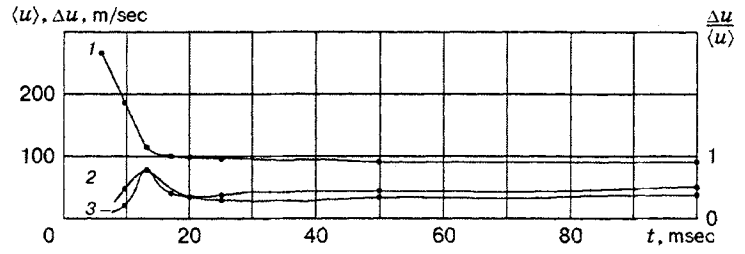

Fig. 5. Variation of the mean and vortex components of the flow velocity and their relative values in the transient and steady regimes ($r = 80$ mm, $z = 7.5$ mm, $V_r = 80$ liters): curves 1–3 refer to $\langle u\rangle$, Δu, and $\Delta u/\langle u\rangle$, respectively.

Bernoulli integral. It should be noted that different streamlines belonging to different vortices pass through the probe at the instants of registration of the pressure maximum and minimum, and the flow enthalpies on them (Bernoulli integrals) are also different.

Thus, for the extreme values of velocity, we can write

$$\langle u\rangle + \Delta u = \{[2\gamma/(\gamma-1)](P_{0\max}/\rho_{0\max})[1-(P_{\min}/P_{0\max})^{(\gamma-1)/\gamma}]\}^{1/2},$$

$$\langle u\rangle - \Delta u = \{[2\gamma/(\gamma-1)](P_{0\min}/\rho_{0\min})[1-(P_{\max}/P_{0\min})^{(\gamma-1)/\gamma}]\}^{1/2}.$$

Eliminating $\langle u\rangle$, we obtain

$$\Delta u = (1/2)\{[2\gamma/(\gamma-1)](P_{0\max}/\rho_{0\max})[1-(P_{\min}/P_{0\max})^{(\gamma-1)/\gamma}]\}^{1/2}$$

$$-(1/2)\{[2\gamma/(\gamma-1)](P_{0\min}/\rho_{0\min})[1-(P_{\max}/P_{0\min})^{(\gamma-1)/\gamma}]\}^{1/2}.$$

Eliminating Δu, we find $\langle u\rangle$ using the formula

$$\langle u\rangle = (1/2)\{[2\gamma/(\gamma-1)](P_{0\max}/\rho_{0\max})[1-(P_{\min}/P_{0\max})^{(\gamma-1)/\gamma}]\}^{1/2}$$

$$+(1/2)\{[2\gamma/(\gamma-1)](P_{0\min}/\rho_{0\min})[1-(P_{\max}/P_{0\min})^{(\gamma-1)/\gamma}]\}^{1/2},$$

where $P_{0\max}$, $P_{0\min}$ and $P_{\max}$, $P_{\min}$ are the maximum and minimum total pressures (stagnation pressures) and static pressures registered by the probes, respectively, $\rho_{0\max}$ and $\rho_{0\min}$ are the maximum and minimum stagnation densities, and $\gamma = 1.4$ is the ratio of specific heats. Taking into account the condition of isentropic flow, we can replace the ratios $P_{0\max}/\rho_{0\max}$ and $P_{0\min}/\rho_{0\min}$ by $(P_{0\max}/\langle\rho_0\rangle)(\langle P_0\rangle/P_{0\max})^{1/\gamma}$ and $(P_{0\min}/\langle\rho_0\rangle)(\langle P_0\rangle/P_{0\min})^{1/\gamma}$, respectively, where $\langle P_0\rangle = (P_{0\max}+P_{0\min})/2$ and $\langle\rho_0\rangle$ are the mean stagnation pressure and density. In this case, the values of $\langle\rho_0\rangle$ and Δu are determined by five measured quantities: stagnation temperature of the flow T_0 [9], $P_{0\max}$, $P_{0\min}$, $P_{\max}$, and $P_{\min}$. A comparison of oscillation phases showed that the values $P_{0\max}$ corresponded to $P_{\min}$, and vice versa. The reason for the error in calculating Δu is that the pressure values are registered by an S9-16 oscillograph at separate time instants, and this error increases with decreasing amplitude of oscillations. According to our estimates, it does not exceed 15%.

Variations of $\langle u\rangle$, Δu, and $\Delta u/\langle u\rangle$ in time at the point $r = 80$ mm, $z = 7.5$ mm and for air exhaustion from a receiver with volume $V_r = 80$ liters are shown in Fig. 5. The absolute value of Δu and the relative value of $\Delta u/\langle u\rangle$ have maxima in the transient regime and decrease and stabilize when the flow regime becomes steady. Figure 6 shows the distribution of the examined quantities along the chamber radius and axis in the transient and steady regimes ($t = 10$ and 100 msec and $z = 7.5$ mm). The oscillations increase with decreasing radius in the region of quasi-solid rotation of the flow, and then decrease in the region of the potential vortex. The profile of the curve $\Delta u/\langle u\rangle$ is similar to the profile of Δu. During the entire transient process, the behavior of the examined quantities remains qualitatively similar. We note the equality of the velocities $\langle u\rangle$ and Δu in the region $r = (2/3)R \approx 70$ mm, which follows from the equality of the pressures $P_{0\min} = P_{\max}$, i.e., the flow stops if the directions of these velocities are opposite. The values of Δu and

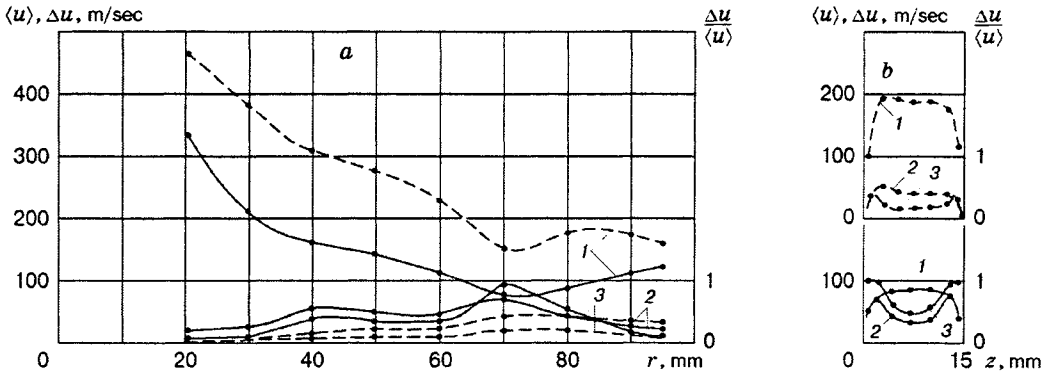

Fig. 6. Variation of the mean and vortex components of the flow velocity and their relative values along the chamber radius and axis in the transient and steady regimes ($z = 7.5$ mm and $V_r = 80$ liters): $t = 100$ (solid curves) and 10 msec (dashed curves); curves 1–3 refer to $\langle u \rangle$, Δu, and $\Delta u/\langle u \rangle$, respectively.

$\Delta u/\langle u \rangle$ increase along the chamber axis z when approaching the walls. In the steady regime, we have $\Delta u/\langle u \rangle = 1$ for $z = 3$ mm in the region $r = 80$ mm. We also note that the estimate of Δu for the point $r = 80$ mm made above by approximate differentiation of the equation of motion is little different from that calculated using the Bernoulli equation (see Figs. 5 and 6).

Conclusions. 1. A vortex flow structure with the characteristic size of the vortices of 1/10–1/20 of the primary vortex has been experimentally observed in a planar-radial vortex chamber for the first time. The vortex axes are perpendicular to the butt-end walls of the chamber. An interpretation of the vortex structure of the flow is proposed.

2. The vortex component of velocity in the flow core along the chamber radius and axis has been calculated. In the steady regime, its maximum values are reached at a distance of about 2/3 of the chamber radius (at the boundary of quasi-solid rotation and potential vortex).

This work was supported by the Russian Foundation for Fundamental Research (Grant No. 96-02-19121a).

REFERENCES

1. G. J. Ranque, "Method and apparatus for obtaining from fluid under pressure two currents of fluids at different temperatures," USA Patent No. 1,952,281 (1934).
2. A. P. Merkulov and V. M. Kudryavtsev, "Turbulence and its role in the vortex effect," in: *Some Aspects of Studying the Vortex Effect and its Industrial Application*: Proc. I All-Union Conf. (Kuibyshev, 1972), Kuibyshev Aviats. Inst., Kuibyshev (1974), pp. 31–39.
3. M. E. Deich, *Technical Gas-Dynamics* [in Russian], Énergiya, Moscow (1974).
4. S. V. Lukachev, "Unsteady gas-flow regimes in a vortex Ranque tube," *Inzh.-Fiz. Zh.*, **41**, No. 5, 784–790 (1981).
5. S. V. Lukachev, "Formation of coherent vortex structures in a vortex Ranque tube," in: *Vortex Effect and its Application in Technology*: Proc. IV All-Union Conf. (Kuibyshev, 1983), Kuibyshev Aviats. Inst., Kuibyshev (1984), pp. 38–44.
6. B. I. Zaslavskii and B. V. Yur'ev, "Flow structure in a planar vortex chamber," *Prikl. Mekh. Tekh. Fiz.*, **39**, No. 1, 84–89 (1998).
7. F. A. Bykovskii and E. F. Vedernikov, "The flow in a planar-radial vortex chamber. 1. An experimental study of the velocity field in transient and steady flows," *Prikl. Mekh. Tekh. Fiz.*, **40**, No. 6, 112–121 (1999).
8. A. N. Petunin, *Methods and Equipment for Gas-Flow Measurement* [in Russian], Mashinostroenie, Moscow (1972).

9. V. G. Makarenko and V. F. Tarasov, "Experimental model of a tornado," *Prikl. Mekh. Tekh. Fiz.*, **28**, No. 5, 115–122 (1987).
10. V. G. Makarenko, "Dependence of formation time of oscillating vortices on excitation frequency of a rotating fluid," *Prikl. Mekh. Tekh. Fiz.*, **36**, No. 1, 85–94 (1995).
11. D. G. Akhmetov and V. F. Tarasov, "Structure and evolution of vortex cores," *Prikl. Mekh. Tekh. Fiz.*, **27**, No. 5, 68–73 (1986).
12. G. Schlichting, *Boundary Layer Theory*, McGraw-Hill, New York (1968).
13. L. I. Sedov, *Mechanics of Continuous Media* [in Russian], Vol 2, Nauka, Moscow (1973).
14. I. I. Smul'skii, "Specific features of velocity and pressure measurement in a vortex chamber," in: *Thermophysics and Physical Hydrodynamics* (collected scientific papers), Inst. of Thermal Phys., Sib. Div., USSR Acad. of Sci., Novosibirsk (1978), pp. 125–132.